# High-resolution optical spectroscopy of YAG:Nd: A test for structural and distribution models

V. Lupei, A. Lupei, C. Tiseanu, S. Georgescu, C. Stoicescu, and P. M. Nanau
*Institute of Atomic Physics, 76900 Bucharest, Romania*
(Received 5 July 1994; revised manuscript received 13 September 1994)

Results are presented on the multisite structure of $Nd^{3+}$ in YAG, obtained from a comparative study of melt-grown high-temperature (HT) and flux-grown (F) crystals by using optical spectroscopy in connection with x-ray data. Absorption and emission data by pumping into $^4G_{5/2}$, $^4F_{9/2}$, and $^4G_{7/2}$ $Nd^{3+}$ multiplets are presented; very good resolution is obtained for pumping into $^4F_{9/2}$. The optical spectra show three types of centers: centers present in all samples, centers present mainly in the HT crystals (and very weak in F samples), and minor or irregular centers. Besides the main center ($Nd^{3+}$ in isolated dodecahedral $c$ sites) all samples contain three satellites, assigned to $Nd^{3+}(c)$-$Nd^{3+}(c)$ pairs in the first, second, and third coordination spheres. A model is proposed to explain the pair lifetimes and their dependence on Nd concentration by assuming a superexchange interaction for the nearest-neighbor pair and electric dipole coupling for the other pairs. Three satellites of equal intensities, observed in the HT samples (and very weak in the F crystals), are connected with the crystal-field perturbations at the $c$ sites produced by an excess of $Y^{3+}$ ions in octahedral $a$ sites, as predicted by the nonstoichiometry data. This result is consistent with the very weak intensity and with the systematic equivalence of the {222} forbidden reflections in our x-ray data, obtained only in the HT crystals. Arguments are given that these satellites are involved in cross-relaxation processes similar to those of the main center. The spectral features of a center that dominates the low-temperature $^4F_{3/2}$ emission under pumping at 532 nm are also analyzed.

## I. INTRODUCTION

Doping of garnet crystals with rare earths ($R^{3+}$) is expected to lead to the appearance of a very limited variety of structural centers, according to the site preference of the dopant. However, a much more complex behavior is observed in optical spectra. The multisite structure of $R^{3+}$ in garnet crystals is still an incompletely elucidated problem; the analysis of this structure requires further attention due to the structural information that could be obtained, the data on the $R^{3+}$-$R^{3+}$ interaction mechanisms, and its possible role in quantum efficiency [as has been discussed for $Nd^{3+}$ in yttrium aluminum garnet[1-3] (YAG)].

The ideal structure of the simple rare-earth garnets $A_3B_2C_3O_{12}$ is cubic and the unit cell contains eight molecular units. In these garnets all the cations are trivalent; $A$ are rare-earth or group-III elements located at dodecahedral $c$ sites (of local $D_2$ symmetry), while $B$ and $C$ are group-III elements such as $Al^{3+}$ or $Ga^{3+}$. The ions $B$ are placed in trigonally distorted octahedral $a$ sites ($C_{3i}$ symmetry), while $C$ ions occupy tetrahedral $d$ sites ($S_4$ symmetry). High-accuracy analyses[4,5] have shown that the composition of garnet crystals grown from melt [high-temperature (HT) crystals] departs from the ideal stoichiometric ratio, showing an excess (several percent as a function of composition) of element $A$; this is usually not observed in the low-temperature flux-grown (F) crystals.

Previous investigations[6-8] have separated the $R^{3+}$ optical spectra in garnets into: (i) the main spectrum corresponding to $R^{3+}$ in nonperturbed dodecahedral $c$ sites, the prevailing $N$ lines; (ii) satellites showing dopant-concentration dependence of the relative intensities and assigned to the near-neighbor (NN) pairs of $R^{3+}$ ions in $c$ sites, $M$ lines; (iii) satellites whose relative intensity does not depend on $R^{3+}$ content, present in HT crystals and assigned to $c$ sites perturbed by the presence of $A$ ions in anomalous $a$ sites, $P$ lines; and (iv) weak lines assigned to $R^{3+}$ in octahedral $a$ sites, $A$ lines. The validity of this model was tested[6-8] by codoping with small amounts of $Sc^{3+}$ ions which occupy octahedral $a$ sites. The analysis of the site-selective excitation spectra and of the temporal behavior of luminescence[3,9,10] confirmed this model. An alternative model,[1,2] based on selective excitation of five nonequivalent $Nd^{3+}$ sites, assumes as sources of perturbation anionic impurities such as $OH^-$.

The number of reported satellites depends not only on the ion or optical transition, but also on the investigation techniques. Most of the recent data refers to site-selective laser spectroscopy. Although this technique is superior to others as concerns the resolution, it could give misleading information about the relative intensities of various satellites. Thus, the information on the distribution of the activators contained in the luminescence data could be "filtered" by selective pumping, saturation, reabsorption, or energy-transfer quenching effects; in this respect the high-resolution absorption data are more accurate.

Despite the general acceptance of the cubic symmetry for the simple garnet crystals, a slight deviation from cubic symmetry of several garnet crystals (such as $Gd_3Ga_5O_{12}$, $Gd_3Fe_5O_{12}$, and $Y_3Fe_5O_{12}$) was inferred from x-ray data,[11] based on the occurrence of weak-intensity {222} reflections, forbidden in the $Ia3d$ group. To our

 

knowledge, no experiments on {222} reflections in $Y_3Al_5O_{12}$ have been reported. Recently,[12,13] by extended x-ray-absorption fine-structure spectroscopy (EXAFS), it has been directly demonstrated that in many garnets (including YAG) some of the *A* lanthanide ions enter into an octahedral environment. However, since the estimated fraction of *A* ions in octahedral sites (up to 9%, almost independent of the garnet chemical composition) was larger than that given by nonstoichiometric data, a fraction of about 13.5% of the *B* atoms was assumed to enter in dodecahedral *c* sites. These results were connected with the x-ray forbidden reflections to explain a global deviation from cubic symmetry of garnets.

The present paper contains a deeper investigation of $Nd^{3+}$ multisite structure in HT- and F-grown YAG, obtained by optical spectroscopy (high-resolution transmission and site-selective emission spectra at various temperatures and dopant concentrations); these data are discussed in connection with x-ray data on the same samples. The structural information is compared with recently published EXAFS data. The energy-transfer processes involving various satellites are also analyzed.

## II. EXPERIMENT

Various YAG:Nd samples grown from high-purity (99.999%) raw materials by high-temperature techniques, Czochralski or Bridgman, with concentrations from 0.1 to 2.5 at. % $Nd^{3+}$, have been investigated. Flux-grown samples containing $Nd^{3+}$ and $Cr^{3+}$ have also been studied. The spectra have been measured with a 1-m double monochromator (GDM-1000) and a cooled S-20 photomultiplier. For excitation a tungsten-halogen lamp and a Quantel IV YAG dye laser have been used. A PAR phase-sensitive system and a PAR 162 boxcar averager have been used for detection. The x-ray diffraction data have been measured at room temperature with a TUR M62 spectrometer.

## III. RESULTS

### A. X-ray data

In flux-grown (900–1250 °C) samples only the diffraction peaks corresponding to the $Ia3d$ group have been observed. In HT (1970 °C) Czochralski or Bridgman crystals, besides the reflections that could be indexed by $Ia3d$, weak lines corresponding to {222} reflections are observed. In the limit of experimental errors, these reflections have similar, very small intensities, for all [111] directions, unlike the data reported for other oxide garnets[11] where one of these reflections was systematically larger (up to a factor of about 3) than the other three. These reflections are at least two orders of magnitude weaker than the $Ia3d$ reflections.

### B. Transmission spectra

The transmission spectra in several spectral regions have been investigated, with special attention to absorption in $^4F_{3/2}$, the emitting level, and to $^4F_{9/2}$, $^4G_{5/2}$, and $^4G_{7/2}$, used as pump levels. They consist of main lines and of a series of satellites. As reported before,[6–8] the satellite structure is different for high-temperature-grown crystals and low-temperature (flux) ones. The resolution of satellites depends on the multiplet and it is higher for the transitions between the lowest Stark components of multiplets. No differences between Czochralski and Bridgman samples have been noticed.

The main features of the spectra are similar to those reported earlier:[6–8] the main line *N*, two *P* satellites ($P_1$ and $P_2$), and one *M* satellite, which we shall denote in what follows by $M_1$. Besides this large-scale-resolved structure, a small-scale satellite structure is reported in this work. A representative transmission spectrum at low temperatures for the $^4I_{9/2}(1)\rightarrow{}^4F_{3/2}(1)$ $Nd^{3+}$ transition in YAG, for a sample with ~1 at. % Nd grown by the Czochralski (HT) method, is given in Fig. 1(a). The intensities of $P_1$ and $P_2$ are equal and their relative intensity with respect to *N* is practically independent of $Nd^{3+}$ concentration *C* (and represents about 2.3–2.7 %, for each of them), while that of the satellite $M_1$ shows a $4C$ dependence. Though we could not measure the intensities of other lines, due to the lack of resolution, from the dependence on *C* we could distinguish two *M*-type satellites close to the main line ($M_2$ at about $+1$ $cm^{-1}$ from the main line *N* and with intensity about twice that of $M_1$, and $M_3$ weaker than $M_1$ at about $-1.2$ $cm^{-1}$ from *N*) and a *P* satellite; this assignment is confirmed by emission spectra. These lines are present in all the HT crystals. Additional very weak absorption lines $S_i$ are observed, some of them in all samples (Table I), others with irregular appearance. In the flux-grown samples the sa-

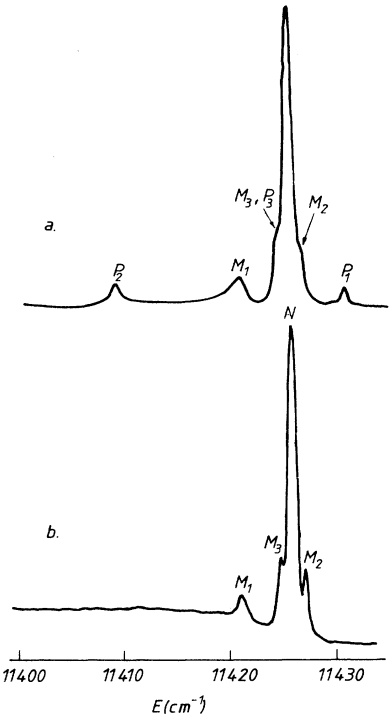


FIG. 1. Transmission $^4I_{9/2}(1)\rightarrow{}^4F_{3/2}(1)$ spectra for YAG:Nd (1 at. %) at 30 K. (a) Czochralski-grown crystals and (b) flux crystals.

TABLE I. Satellite structure of Nd in YAG.

| Site | Position in $^4F_{3/2}$ ($cm^{-1}$) | Position in $^4F_{9/2}$ ($cm^{-1}$) | Samples |
|---|---|---|---|
| $P_1$ | 11 430.8 | 14 630 | HT |
| $M_2$ | 11 426.5 | 14 627.5 | HT, F |
| $N$ | 11 425.5 | 14 626.5 | HT, F |
| $M_3$ | 11 424.7 | 14 623.5 | HT, F |
| $P_3$ | 11 424.2 | 14 622.5 | HT |
| $M_1$ | 11 420.5 | 14 619 | HT, F |
| $P_2$ | 11 409 | 14 616.5 | HT |
| $S_1$ | 11 415 | 14 617.5 | HT |
| $S_2$ | 11 413 | 14 623 | HT |
| $S_3$ | 11 406.5 | 14 614 | HT |
| $A$ | 11 39514 | 14 600 | HT |

tellites $P$ are very weak (at least one order of magnitude weaker than in the HT crystals) and the lines $N$ and $M$ are sharper. Figure 1(b) presents the transmission spectrum of a $F$ sample with $\sim 1$ at. % $Nd^{3+}$: the satellites $M_2$ and $M_3$ are more evident than in HT crystals.

We obtained very good resolution for the low-temperature transmission spectra corresponding to the $^4I_{9/2}(1) \rightarrow {}^4F_{9/2}(1)$ transition. Three $P$-type satellites with equal intensity are clearly resolved in this transition, as shown in Figs. 2(a), 2(b), and 2(c) for HT crystals with different Nd content; the $P$ lines are very weak in the flux crystals [Fig. 2(d)]. The three concentration-dependent $M$ satellites are clearly resolved in all samples. One must remark the presence of $M$ satellites even at very low concentrations.

The satellite structure of $^4G_{5/2}$ shows a much poorer resolution and this is the reason for nonselectivity of the previous site-selective experiments[1,2,10,14,15] performed by pumping in this level.

A noticeable difference between the transmission spectra of the HT and F crystals has also been observed in the case of the $^4I_{9/2} \rightarrow {}^4G_{7/2}$ transition, the range that encompasses the wavelength of the second harmonic of a YAG:Nd laser. The spectra of the flux-grown YAG:Nd crystals show, at low temperatures, four lines that correspond to transitions from the lowest Stark component of $^4I_{9/2}$ to the four components of $^4G_{7/2}$ of the main center $N$, and several shoulders, especially for the $1 \rightarrow 1$ transition, far from 532 nm. At low temperatures the HT crystals show, besides these lines and a series of shoulders, a sharp and fairly strong absorption at 18 804 $cm^{-1}$ [line $A$ in Fig. 3(a)]. With increasing temperature the intensity of this line decreases and above 200 K it cannot be observed; at the same time other lines broaden and hot bands (temperature-activated transitions) appear. Of interest for 532-nm pumping is the $3 \rightarrow 4$ transition of the main center $N$, at 18 788 $cm^{-1}$ [Fig. 3(b)]. This temperature dependence must be considered in the analysis of emission spectra with pumping at 532 nm.

### C. Luminescence spectra

The luminescence spectra from $^4F_{3/2}$ have been excited either with a tunable dye laser in the region of $^4F_{9/2}$ or $^4G_{5/2}$ absorption or with a frequency-doubled YAG:Nd laser in the region of $^4G_{7/2}$ absorption.

#### *1. Emission under excitation in $^4F_{9/2}$*

The remarkable resolution of the $^4F_{9/2}$ absorption spectrum at low temperatures enables the selective excitation of emission from most of the centers observed in absorption. Thus, Fig. 4 shows the $^4F_{3/2}(1) \rightarrow {}^4I_{9/2}(1)$ emission lines obtained by pumping in $N$ line and $P_i$ satellites in $^4F_{9/2}$. For each excitation only one emission line is obtained; a third $P$ satellite has been obtained in the $^4F_{3/2}(1) \rightarrow {}^4I_{9/2}(1)$ transition, at about only $-0.8$ $cm^{-1}$ form the main line. A clear correspondence between the satellites observed in $^4F_{3/2}$ and $^4F_{9/2}$ can be established; the crystal-field components for various centers have been obtained. At higher temperatures (above 200 K) the lines in absorption and emission spectra broaden to an extent that only the emission of the main center is

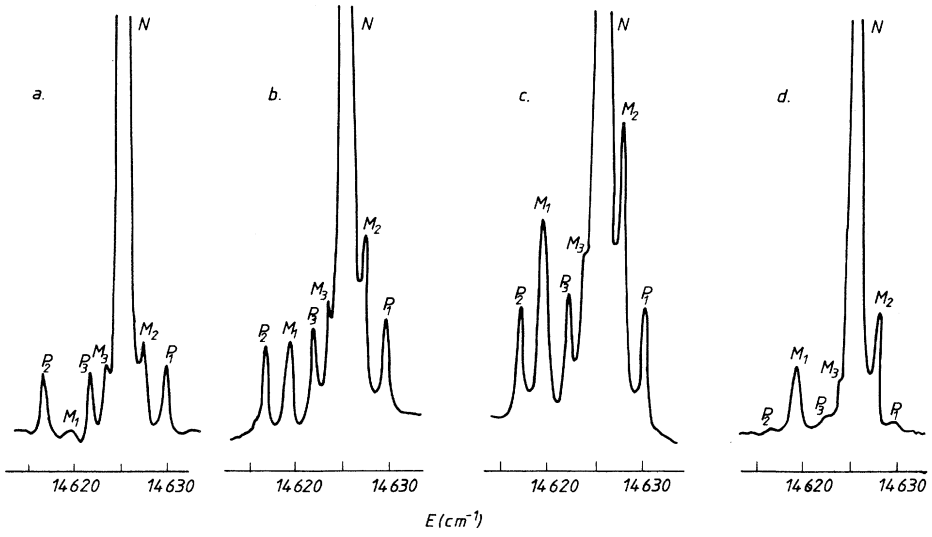


FIG. 2. Transmission $^4I_{9/2}(1) \rightarrow {}^4F_{9/2}(1)$ spectra for YAG:Nd at 30 K. (a)–(c) Czochralski-grown crystals, (a) 0.1 at. % Nd, (b) 0.5 at. % Nd, and (c) 1 at. % Nd; (d) flux crystal, 1 at. % Nd.

observed.

A very important result of this investigation is the observation of emission of the $M_1$ center, assigned to the nearest-neighbor $Nd^{3+}$ pairs and considered previously[6–10] completely quenched. The selective excitation of the $M_1$ satellite in $^4F_{9/2}$ leads to a very short and weak emission at the $M_1$ wavelength in $^4F_{3/2}$. The time-resolved spectra illustrate this behavior. The emission recorded for the most concentrated sample (2.5 at. %) and with a rather large monochromator slit shows, immediately after the pump pulse [Fig. 5(a)], the $M_1$ line together with the lines of two centers simultaneously excited with it ($P_3$ and a minor center with emission at 11 416 $cm^{-1}$) while at a delay of 3 $\mu$sec [Fig. 5(b)], no trace of $M_1$ emission is observed.

### 2. *Emission under selective excitation in $^4G_{5/2}$*

Due to the low resolution of $^4G_{5/2}$ absorption spectra, simultaneous emission from different structural centers is obtained even at low temperatures; this effect is temperature enhanced. The temperature changes of the relative intensities of emission from various centers, at a given pumping wavelength, have been previously explained[1,2,10] by thermally activated energy transfer between various centers. A comparison with the spectra obtained by pumping in $^4F_{9/2}$ rules out this explanation. Above about 200 K the resolution of $^4F_{3/2}$ emission is lost and only the main-line emission is recorded. As in the case of excitation in $^4F_{9/2}$, time-resolved spectroscopy is useful to separate the emitting centers. This is illustrated in Fig. 6, where the emission spectra at two delay times (0 and 200 $\mu$sec) from the laser pulse are presented. Due to the lower resolution in pumping, the emission of $N$ and $P_1$ is simultaneously excited with $M_2$; but, while the first centers have similar lifetimes, $M_2$ has clearly a much shorter one.

### 3. *Excitation at 532 nm*

At pumping at 532 nm the $Nd^{3+}$ emission spectra at 300 K are very complex and cover a large wavelength range from about 380 nm to infrared. The emission originates from at least two metastable levels, whose lifetimes at low concentrations are about 3 and 260 $\mu$sec, respectively: the $(^2F2)_{5/2}$ level, excited by a two-photon adsorption process, as observed previously,[16] and $^4F_{3/2}$ excited

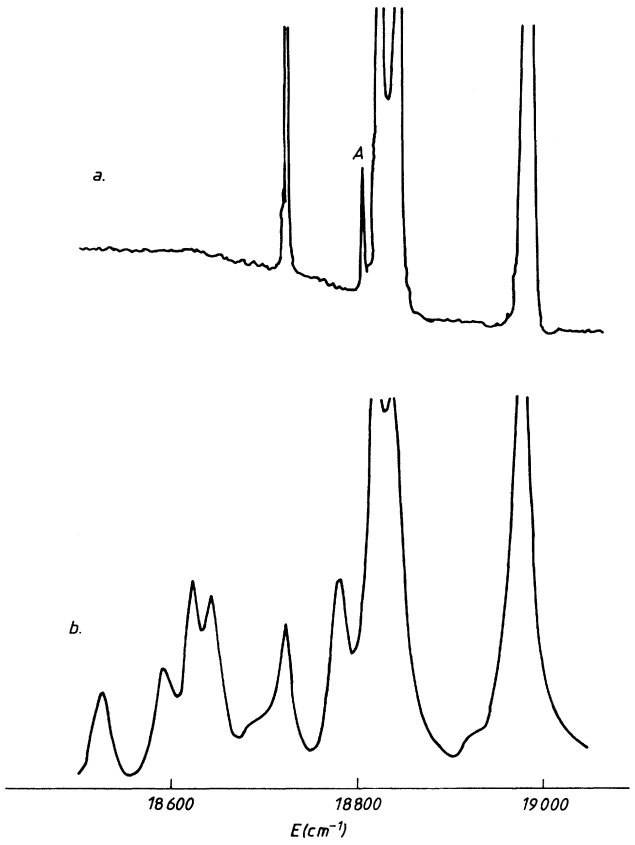


FIG. 3. Temperature dependence of $^4I_{9/2} \rightarrow {}^4G_{7z2}$ in Czochralski-grown YAG:Nd (1 at. %) spectra measured at (a) 30 K, (b) 300 K. The line $A$ is at 18 804 $cm^{-1}$.

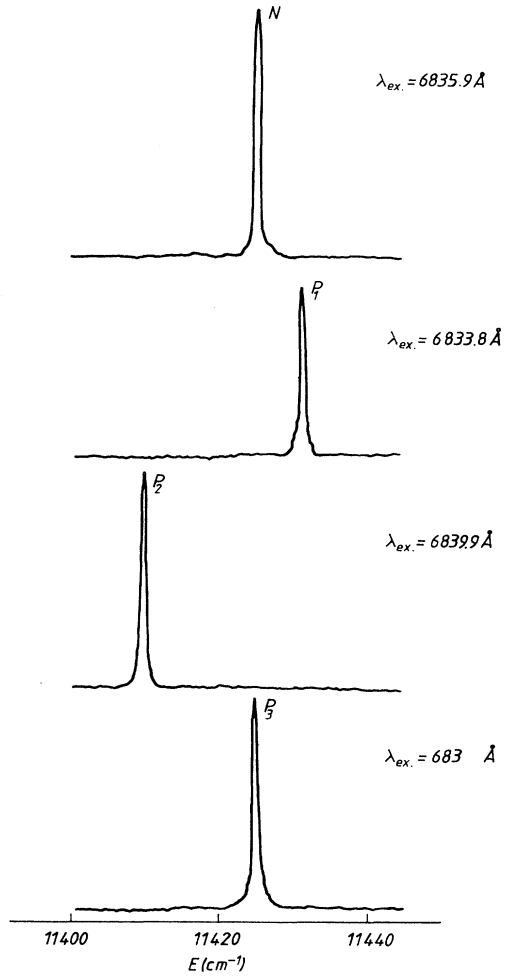


FIG. 4. $^4F_{3/2}(1) \rightarrow {}^4I_{9/2}(1)$ emission of selectively excited (into $^4F^{9/2}$) $N$ and $P_i$ centers in Czochralski-grown YAG:Nd (1 at. %).

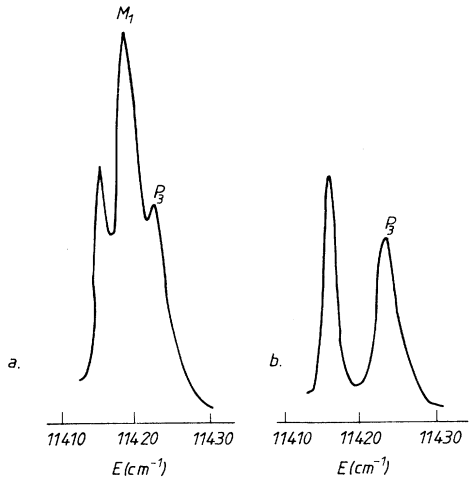


FIG. 5. Time-resolved $^4F_{3/2}(1) \rightarrow {}^4I_{9/2}(1)$ emission in the region of $M_1$ satellite in a YAG:Nd (2.6 at. %) sample recorded (a) after the laser pump pulse into $^4F_{9/2}$, and (b) at 3 $\mu$sec after the pump pulse.

directly by a one-photon process or as a consequence of the two-photon process. The emission spectra correspond to the unperturbed $N$ center; at 300 K the pumping occurs in a temperature-activated absorption of $N$, $[^4I_{9/2}(3) \rightarrow {}^4G_{7/2}(4)]$, and the relative contribution from absorption of other structural centers is negligible. A very weak emission around 810 nm from $^4F_{5/2}$ could be observed at this temperature as in Ref. 17.

The $^4F_{3/2}$ emission under 532-nm pumping is strongly temperature dependent and it is different in HT and F crystals (Fig. 7). The $N$-center emission drops in intensity as the temperature decreases and in HT-grown YAG and

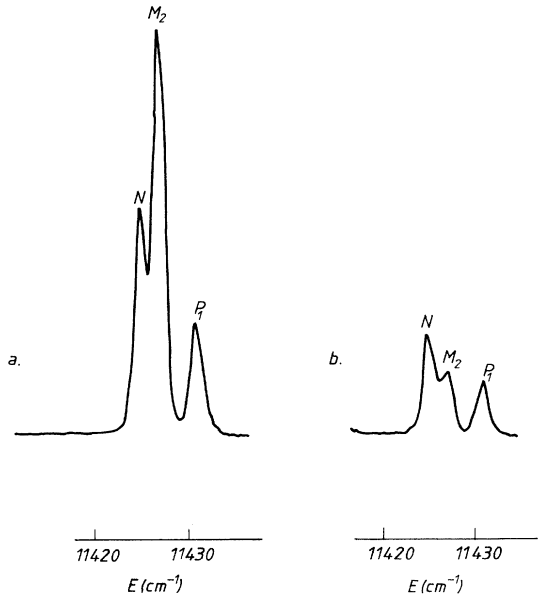


FIG. 6. Emission spectrum in the region of $M_2$ satellite in YAG:Nd (1 at. %) under quasiselective pumping into $^4G_{5/2}$ (a) after the laser pulse, and (b) at 200 $\mu$sec after pumping.

under $\sim$200 K the emission from all the other satellites observed in absorption, excepting $M_1$, becomes apparent. Under about 150 K a different emission center ($A$) is observed; it becomes the main feature of the emission under 77 K. The emission allows the determination of some energy levels connected with this center, $^4F_{3/2}(1) \sim 11\,395$ cm$^{-1}$ (at $-30$ cm$^{-1}$ from the main line $N$) and $^4I_{9/2}$ at 0, 115, 212, 354, and 860 cm$^{-1}$. The 11 395-cm$^{-1}$ emission has been observed previously,[18] in the low-temperature spectra of YAG:Nd:Cr under 532-nm pumping, and assigned to the unperturbed $N$-center emission. We note that absorption is negligible at 11 395 cm$^{-1}$ and the main $N$-center absorption (or emission) to $^4F_{3/2}(1)$ lies at 11 425.5 cm$^{-1}$. The center $A$ has lifetime and concentration quenching similar to $N$, but it is a particular center and could probably be connected with the 18 804-cm$^{-1}$ absorption line of $^4G_{7/2}$ in the HT samples, which is very close to the 532-nm pumping wavelength. This absorption line and the $A$-center emission are absent in flux samples, another fact that supports their connection. We mention that the emission of this center was observed together with other minor centers by pumping in $^4F_{9/2}$ too.

At this pumping, besides the $Nd^{3+}$ emission, several broadbands, sample dependent, have been noticed. These broadbands could be due to impurities (such as $Cr^{3+}$,$Fe^{3+}$,$Ti^{3+}$) present accidentally in some of the investigated samples.

### D. Luminescence decays

The kinetics of $^4F_{3/2}$ population of various emitting $Nd^{3+}$ centers has been investigated by monitoring the temporal evolution of emission after the exciting laser pulse (10 nsec); the resolution is reduced in some instances by insufficient resolution of the spectra. An important feature of the temporal behavior of $^4F_{3/2}$ emission under pumping with dyes or the second harmonic of YAG:Nd is the absence of an obvious rise time. This indicates a predominantly direct excitation of $^4F_{3/2}$ by rapid phonon relaxation from the pump level.

Generally, the observed centers could be classified according to their temporal behavior into two groups: (i) centers with Nd concentration-dependent nonexponential decays similar to those of $N$, and (ii) centers with much faster decays.

The first group contains the $N$, $P_i$, $A$, and some of the $S_i$ centers. As discussed in previous reports,[3,19] the concentration-dependent nonexponential decays of the $N$ center are due to energy transfer by cross relaxation on intermediate levels $^4I_{13/2}$ and $^4I_{15/2}$ inside the $Nd^{3+}$ system. The similarity of the decays of $P_i$ and $A$ centers to that of $N$ suggests that for these centers similar cross relaxations occur, the system of acceptors containing practically all the $Nd^{3+}$ ions from the system.

The second group of centers contains the satellites $M_i$. As mentioned above, the enhanced pumping resolution into $^4F_{9/2}$ enables the observation of emission of the $M_1$ center: the decay is extremely fast with a lifetime of the order of a few tenths of microseconds and thus the emission cannot be observed if the temporal resolution of the equipment is low. If the pumping is not selective enough,

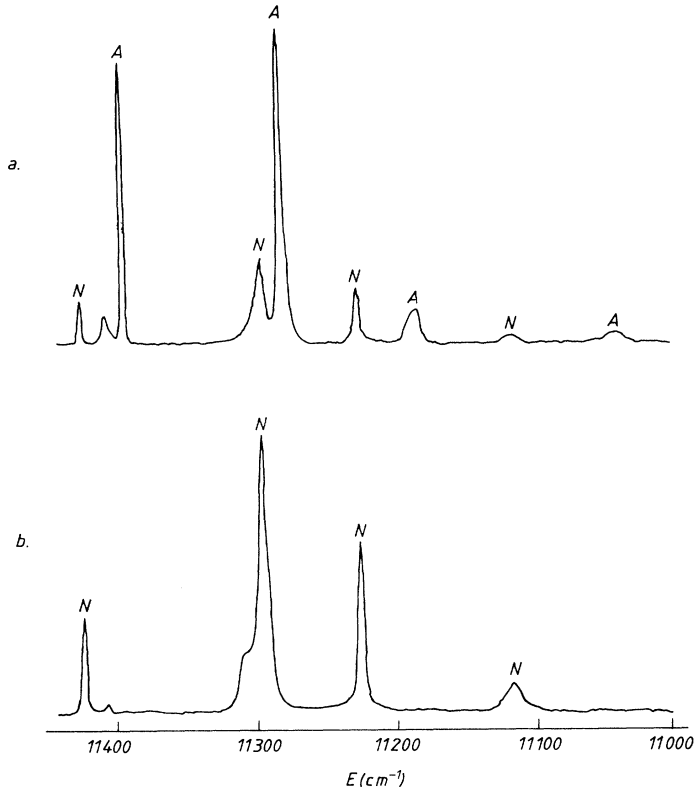


FIG. 7. Low-temperature (30 K) $^4F_{3/2} \rightarrow {}^4I_{9/2}$ emission in YAG:Nd (1 at.%) under pumping at 532 nm. (a) Czochralski sample, and (b) flux sample.

the very low quantum efficiency makes unlikely the observation of $M_1$ emission in the luminescence experiments. The luminescence emission of $M_2$ shows a fast nonexponential decay with an effective lifetime dependent on concentration, about 95 $\mu$sec at 0.5 at. % Nd and 40 $\mu$sec at 2.5 at. % Nd. The emission of $M_3$ could not be resolved completely; its apparent lifetime at low Nd concentration lies in the range 130–140 $\mu$sec, evidently lower than for center $N$.

## IV. DISCUSSION

### A. The crystallographic structure of the rare-earth garnets

Different experimental data (chemical composition, structural investigations) have suggested that the composition and structure of the garnets could differ from the ideal $A_3B_2C_3O_{12}$, where $A$, $B$, and $C$ ions occupy only the $c$, $a$, and $d$ sites, respectively. Thus, the nonstoichiometric model[4,5,8,20] considers that in garnets (especially the HT crystals) there is an excess of $A$ ions which enter into octahedral sites, and the composition can be written as $A_3(B_{1-x}A_x)_2C_3O_{12}$. An analysis of published data shows that the fraction $x$ depends exponentially on "octahedral" radii $r_A$ and $r_B$ (expressed in nm) as $x \sim C_1 \exp[-C_2(r_A^3 - r_B^3)]$, where $C_1$ is a crystal-growth-temperature-dependent parameter and $C_2 \sim 16.75 \times 10^{-3}$ nm. For YAG crystals grown from the melt (1970 °C) the fraction $x$ of $a$ sites occupied by $Y^{3+}$ ions, determined from chemical analysis, is about 0.015–0.020. The measurements of this fraction for diluted rare-earth dopants in $Ho_3Fe_5O_{12}$ show that it is practically independent of their ionic radius.[20] Thus we could expect for rare-earth ions introduced in low concentration in YAG a value of $x$ similar to that of $Y^{3+}(a)$.

Our x-ray data on HT- and flux-grown YAG crystals do not give grounds to assume a global symmetry lowering and suggest that the forbidden {222} reflections (having similar intensities in HT crystals and missing in flux samples) originate rather from local defects in these planes, normally occupied only by $Al^{3+}(a)$ ions. These defects, with a random distribution, are very likely $Y^{3+}(a)$.

### B. Distribution of activators and defects in crystals

Substitution of trivalent $A$ ions by $R^{3+}$ activators does not require charge compensation, and therefore there is no reason for electrostatic-interaction correlation in their distribution in the lattice. Since at low dilution the difference in the ionic radii between $R^{3+}$ and the host cation $A$ does not lead normally to size correlation, the most likely model for $R^{3+}$ distribution in garnets is random uniform occupancy of the available sites. Similar arguments are valid for defects such as anomalous $A$ ions in octahedral sites. This may not be valid when several activators or defects are simultaneously present in the crystals.

For a random uniform distribution of activators the probability of occurrence of ensembles formed by a given activator ion with $n$ neighbor activators in a sphere with $m$ sites is given by

$$C_{nm}=\frac{m!}{n!(m-n)!}C^{n+1}(1-C)^{m-n}\ , \tag{1}$$

where $C$ is the concentration of activators; this shows that in fact only $C(1-C)^m$ activators could be considered as isolated; the others enter in ensembles. For low $C$ values, the most probable ensembles are pairs, i.e., $n=1$, which could occur even at very low activator concentrations. The probability of having ensembles of an activator and $n'$ defects placed on a sphere containing $m'$ sites is given by

$$C_{n'm'}=\frac{m'!}{n'!(m'-n')!}C(C')^{n'}(1-C')^{m'-n'}\ , \tag{2}$$

where $C'$ is the concentration of defects.

### C. Structure and distribution effects in the optical spectra of activators in crystals

Substitution of ions $A$ by $R^{3+}$ in garnets can produce large local distortions due to the dimensional mismatch between them. When two ions (or an ion and a defect) are in neighboring sites they can modify the symmetry and strength of the crystal field at each other's site, a perturbation that can produce shifts of the energy levels, i.e., satellites in optical spectra. If the perturbation does not change the selection rules and the oscillator strength as compared with those of unperturbed ions, the intensities of various satellites will reflect the relative concentrations of the perturbing centers. This could be valid for Kramers $R^{3+}$ ions such as $Nd^{3+}$, but it may not be true for non-Kramers ions such as $Tm^{3+}$ or $Pr^{3+}$.

The number of sites in the first three $c$, $a$, and $d$ coordination spheres around a $c$ site and the radii of these spheres for YAG are given in Table II. According to Eq. (1) the concentration of pairs formed by a $Nd^{3+}$ ion with another $Nd^{3+}$ ion from a coordination sphere with $m$ sites is equal to $mC^2(1-C)^{m-1}$. If the perturbation produced at the central $Nd^{3+}$ ion by ions in any of these $m$ sites is identical, a unique satellite will be obtained, and if no alteration of oscillator strength takes place the relative intensity of the pair line to that of unperturbed (isolated) centers is $mC(1-C)^{-1}$, which at low $C$ is equal to $\sim mC$. Taking the data form Table II the expected relative intensities of satellites corresponding to $Nd^{3+}$ pairs at various distances could thus be estimated.

A similar result can be obtained for the concentration of perturbed centers by the presence of $Y^{3+}(a)$ in the first coordination sphere. However, due to the large size difference between $Y^{3+}$ and $Al^{3+}$ ions in YAG, strong distortions of the lattice take place (as revealed by EXAFS) and due to the mutual perturbation with $Nd^{3+}$ the equivalence of these sites could be destroyed. In YAG each $Al^{3+}(a)$ is surrounded by six NN $Y^{3+}$ in $c$ sites; assuming that the equivalence of the perturbation produced by substitution of the central $Al^{3+}$ by an $Y^{3+}(a)$ at these six NN $Y^{3+}(c)$ sites is destroyed, but the inversion around the central $a$ site is still preserved, three different perturbations could be obtained from a $Y^{3+}(a)$ ion at the NN $c$ sites occupied by Nd. In the optical spectra of $Nd^{3+}$ this would produce three satellites and, if the oscillator strength is not modified, the relative intensity of each of these satellites with respect to nonperturbed sites [estimated from (2)] at low concentrations of activators $C$ and defects $C'$ is $\sim\frac{4}{3}C'$, i.e., practically independent of the activator concentration.

### D. Luminescence kinetics

The luminescence quenching of the main $Nd^{3+}$ line and of the various satellites can be expressed as usual by

$$\frac{I}{I_0}=\exp\left[-\frac{t}{\tau_0}-P(t)\right]\ , \tag{3}$$

where $\tau_0$ is the luminescence lifetime of isolated ions ($\tau_0\sim 260$ $\mu$sec for Nd in YAG at 300 K) and $P(t)$ is the transfer function. The transfer function can be calculated taking into account the type of transfer and the distribution of acceptors in the available lattice sites. For a direct transfer and a random uniform distribution of acceptors in the lattice,

$$P(t)=-\sum_i \ln[1-C_A+C_A\exp(-W_i t)]\ , \tag{4}$$

where the sum extends over all the available acceptor sites and $C_A$, the concentration of acceptors, is equal in this case to the Nd concentration. The transfer function $P(t)$ can be exactly calculated if the transfer rates $W_i$ to each of the acceptor ions at the distances $R_i$ from the donor are known. For dipolar coupling this rate is given by

$$W_i=\frac{C_{DA}}{R_i^6}\ , \tag{5}$$

where $C_{DA}$ is the microparameter of interaction that depends on the spectral properties of donors and acceptors. At large times after the laser pulse, when the effect of distant acceptors is manifested, the discrete distribution can be approximated by a continuous one, the sum in (4) can be replaced by an integral, and $P(t)$ for the dipolar electric interaction takes the Förster form $\gamma t^{1/2}$. At short times $P(t)$ can be approximated by a linear function of $t$:

TABLE II. The cationic coordination for $Y^{3+}$ in YAG.

| Ion site | Neighbors | Ion radius (Å) | Sphere I $N$ | Sphere I $r$ (Å) | Sphere II $N$ | Sphere II $r$ (Å) | Sphere III $N$ | Sphere III $r$ (Å) |
|---|---|---|---|---|---|---|---|---|
| | $Y^{3+}(c)$ | 1.02 | 4 | 3.674 | 8 | 5.612 | 2 | 6.00 |
| $Y^{3+}(c)$ | $Al^{3+}(a)$ | 0.53 | 4 | 3.354 | 8 | 5.408 | 8 | 6.874 |
| | $Al^{3+}(d)$ | 0.39 | 2 | 3.00 | 4 | 3.674 | 8 | 5.612 |

$$P(t)=C_A C_{DA}\sum_i R_i^{-6}t \ . \tag{6}$$

These equations describe the decay of the ensemble of donors; however, if the satellites corresponding to various pairs can be spectrally resolved, the decay can be exactly described for each subensemble. Thus, in the case of NN Nd pairs the temporal evolution of the emission can be described by

$$\frac{I_1}{I_1(0)}=\exp\left[-\frac{t}{\tau_0}\right]\exp(-W_1 t)\exp[-P_1(t)] \ , \tag{7}$$

where $W_1$ is the transfer rate inside the first NN pair, and $P_1(t)$ reflects the transfer to more distant $Nd^{3+}$ ions and is given by

$$P_1(t)=-\sum_{i>m_1}\ln[1-C_A+C_A\exp(-W_i t)] \tag{8}$$

with $m_1$ the number of available sites for $Nd^{3+}$ in the first coordination sphere. If the Nd concentration is not very high the pair decay is quasiexponential, with a lifetime $\tau_1$ given by

$$\tau_1^{-1}=\tau_0^{-1}+W_1 \ . \tag{9}$$

However, if the concentration of acceptors is high, the luminescence decay of this pair will be nonexponential and will show a dependence on acceptor concentration. Thus the emission of the pair center could be regarded as similar to that of a center of intrinsic lifetime $\tau_1$ surrounded by a system of acceptors (such that $i>m_1$) of concentration $C_A$. This treatment is valid when the probability of NN ensembles larger than pairs is negligible; this covers safely the concentration range in our case. A similar description can be given for pairs of any order by a proper choice of $m$. At the same time, the luminescence decay for the ensemble of the remaining centers will be given by Eqs. (3) and (4) with $P(t)$ calculated with a truncated sum which excludes the acceptors involved in resolved satellite pairs. In this case, at the beginning of the decay, $P(t)$ can be approximated by a linear function of time with a slope and duration dependent on truncation. At very large times, $P(t)$ can still be approximated by a Förster law if the truncation is mild; if not, a better description at large times can be obtained by using the continuous distribution approximation for the case of excluded volumes, developed in Ref. 21.

### E. Connection between spectral data and structural models

The transmission and luminescence spectra show that all the investigated samples, regardless of the crystal growth method, contain the center $N$ as the main feature and the satellites $M_i$, whose relative intensity with respect to $N$ depends only on the Nd content. Obviously the center $N$ corresponds to $Nd^{3+}$ in isolated, nonperturbed $c$ sites of YAG. The linear dependence of the relative intensities of the $M$ satellites on $C$, with a factor of 4 for $M_1$, $\sim 8$ for $M_2$, and roughly 2 for $M_3$, suggests that these satellites correspond to pairs formed by a $Nd^{3+}$ ion with $Nd^{3+}$ neighbors from the first ($m=4$), second ($m=8$), and third ($m=2$) $c$ coordination spheres (Table II). This assumption is confirmed by the luminescence decays. Earlier experiments[3,9,10] on YAG:Nd, when no emission from $M_1$ was observed and the satellites $M_2$ and $M_3$ could not be resolved (due to low resolution in the pumping), have shown that the global non-exponential decay could be described by Eqs. (3) and (4) with a dipolar interaction for all acceptors excepting the NN's, where a stronger coupling had to be considered. A transfer microparameter $C_{DA}$ was estimated for the dipolar interaction $\sim 1.85\times 10^{-40}$ $cm^6 s^{-1}$, almost independent of temperature.

If one assumes that $M_2$ and $M_3$ are $Nd^{3+}$ pairs (at 5.6 and 6 Å, respectively) coupled by dipolar interaction, their lifetimes for low $Nd^{3+}$ content can be estimated with relations (9) and (5) and with the microparameter $C_{DA}$ given above as 102 and 128 μsec, respectively. These values are in good agreement with the experimentally estimated lifetimes for a sample with 0.5 at. % Nd (taking into account a possible admixture from the emission of other centers, especially in the case of $M_3$), therefore confirming the assignment based on the statistical random uniform occupancy of $c$ sites by $Nd^{3+}$ ions. This also shows that no evident change of the oscillator strength occurs due to mutual perturbation inside these pairs. We can explain the concentration dependence of $M_2$ and $M_3$ pair decay by using relations (7) and (8) which show that, contrary to the common belief that the ion-pair decays should be exponential, for not very small Nd concentrations, due to energy transfer to more distant ions, the decays become nonexponential and concentration dependent; this effect is difficult to observe if the transfer inside pairs is very fast. We note that a concentration dependence of pair lifetime was also observed for $Pr^{3+}$ in YAG.[22]

As concerns the $M_1$ center in YAG:Nd, the lifetime is of the order of a few tenths of a microsecond; and we could not measure it or its concentration dependence due to the limited resolution of our setup. This short lifetime cannot be explained by a dipolar interaction with the $C_{DA}$ microparameter determined for the other pairs, which would give a lifetime of $\sim 13$ μsec for low $C$; it could be a superexchange interaction as assumed earlier. Two nearest-neighbor $Nd^{3+}$ ions in YAG could be coupled by two $O^{2-}$ bridges, but no such bridges are possible for next-nearest neighbors at 5.6 and 6 Å.

Among the centers appearing regularly in HT but very weak in the flux crystals, we resolved three $P$ satellites, both in $^4F_{9/2}$ absorption and in $^4F_{3/2}$ emission, of equal intensity and with no Nd concentration dependence of the relative intensity. This structure as well as the intensity relative to $N$ (about 2.3–2.7 % of $N$ intensity) corresponds to $C'\sim 0.02$ in the nonstoichiometric model of occupancy of some octahedral sites by $Y^{3+}$ ions, similar with that measured by chemical analysis. The mutual crystal-field perturbation for NN $Nd^{3+}(c)$-$Y^{3+}(a)$ pairs is strong enough to destroy the equivalence of the six $Nd^{3+}(c)$ ions around a $Y^{3+}(a)$ site, but no significant alterations of the oscillator strengths occur. For YAG:$Er^{3+}$ additional $P$ centers[23] assigned to $Y^{3+}(a)$ in

the second coordination sphere were reported. In our case the effect of the other $Y^{3+}(a)$ coordination spheres is not resolved, but it could lead to an inhomogeneous broadening of the lines. We mention also that the model of nonstoichiometric occupancy of $a$ sites by $Y^{3+}$ was successful in explaining the observed satellite structure of $Cr^{3+}$ emission in YAG.[24] Finally, we note that the very low intensity of $P$ satellites in the flux-grown crystals confirms the fact that the degree of departure form stoichiometry in garnets depends on the crystal growth temperature.

For the inversion model[12] proposed from EXAFS data the $Nd^{3+}(c)$ centers could be perturbed by both $Y^{3+}(a)$ and $Al^{3+}(c)$ ions. Thus the perturbations produced by the 13.5% $Y^{3+}(a)$ centers would induce a NN $P$ satellite (or a group of $P$ satellites) of total relative intensity about 35% of that of the $N$ line, while the 9% $Al^{3+}(c)$ centers will produce in the Nd spectra a satellite (or a group) of relative intensity 27% of $N$. No evidence of satellites due to $Al^{3+}(c)$ perturbations was found; thus the optical spectroscopy does not confirm the predictions of the large-scale inversion inferred from EXAFS.[12,13] It is also evident that none of these major satellites could be connected with the perturbing effect of hydroxyl impurities.

An interesting result of this study is the observation of center $A$ (emission at 11 395 $cm^{-1}$) that shows up in all HT crystals. Its appearance and temperature dependence parallel those of the absorption line at 18 804 $cm^{-1}$ in $^4F_{9/2}$, close to 532 nm; this could explain the excitation of the $A$ center and its dominance at low temperatures at this pumping. Emission from $A$ has been obtained also by pumping in other levels, indicating that it is associated with $Nd^{3+}$. The absorption line at 18 804 $cm^{-1}$ and the $^4F_{3/2}$ emission lines of center $A$ are close to those observed for $Nd^{3+}$ in octahedral sites of lithium niobate[25] or in germinates.[26] As discussed above, although the difference between the octahedral radii of $Nd^{3+}$ and $Al^{3+}$ is larger than for $Y^{3+}$, at low dilution some of the $Nd^{3+}$ ions could enter into the octahedral sites of garnets. It would thus be tempting to assign the $A$ emission to such octahedral $Nd^{3+}$ centers. The longer lifetime of the center $A$ as compared to $Nd^{3+}$ in lithium niobate could be explained by a more symmetrical octahedral site in YAG. The quite large intensity of the 18 804-$cm^{-1}$ absorption line (corresponding to a $\Delta J=0$ transition) as compared to the other satellites could be due then to a magnetic dipole transition inside this center.

The luminescence decays of $P$ centers are similar to that of $N$; this indicates that similar energy-transfer processes contribute to the quenching and the acceptors are the same, the total Nd concentration. The selectivity of pumping in $^4F_{9/2}$ enables one to resolve the emission of each center and shows that no other essential intercenter transfers of excitation take place.

Other luminescence emission lines have been obtained either by pumping in the very weak absorption lines or accidentally by pumping the above-discussed centers (especially at pumping in less resolved regions such as $^4G_{5/2}$). Some of these minor centers[2] such as $S_2$ and $S_4$ (Table I), are usually present in HT-grown crystals. The enhancement of absorption or emission from some of the other minor centers was observed in some crystals with traces of transition-metal ions (such as $Cr^{3+}$).

## V. CONCLUSIONS

Improved experimental data on the multisite structure of $Nd^{3+}$ in YAG either in absorption or in emission of high-temperature and flux-grown crystals have been obtained, especially by pumping into the $^4F_{9/2}$ level. This extensive investigation shows the presence of three types of centers, those appearing in all crystals, centers present especially in HT crystals, and minor or irregular centers. All the samples contain, besides the prevailing center $N$, the $M_i$ satellites assigned to $Nd^{3+}(c)$-$Nd^{3+}(c)$ pairs from the first, second, and third coordination spheres. The intensities in absorption and the luminescence decays for these satellites have been explained on the basis of random uniform occupancy of the $c$ sites by $Nd^{3+}$ and by assuming that the crystal-field perturbations do not modify the oscillator strength of the transitions. It was confirmed that the luminescence quenching inside the second- and third-order pairs is a cross relaxation on intermediate $Nd^{3+}$ levels due to an electric dipolar interaction with a microparameter $C_{DA}$ equal to that determined from the nonexponential decay of the global Nd emission.[3,10] A model to explain the nonexponential and concentration-dependent decay for the pairs as an effect of transfer to more distant acceptors is also presented. The luminescence of NN Nd pairs (satellite $M_1$) has been observed due to a good spectral and temporal resolution, and its very short lifetime and quantum efficiency confirm that these pairs are coupled by a strong short-range interaction, probably superexchange, as assumed before. The structure and relative intensities of $P$ satellites confirm the model of random uniform distribution of excess $Y^{3+}(a)$ centers around $Nd^{3+}$ for the degree of nonstoichiometry determined by chemical analysis; they also show that the strong lattice distortion produced by these centers is nonsymmetrical and thus the centers from a given coordination sphere become non-identical. The complete resolution of $^4F_{3/2}$ emission for these satellites shows that no major transfer of excitation between the $Nd^{3+}$ centers exists other than the quenching by cross relaxation and that the results of previous works have been influenced by the accidental, temperature-dependent simultaneous excitation of various centers due to poor resolution of the pumping into the $^4G_{5/2}$ level. No evidence of any major satellite structure to confirm the large-scale inversion model[12,13] inferred form EXAFS or the perturbing effect of hydroxyl[1,2] has been found.

The spectral features of a center $A$ that dominates the low-temperature emission spectra, under pumping at 532 nm, in HT samples have also been analyzed; the possibility of assigning this center to $Nd^{3+}$ in octahedral sites is considered. This work also shows that the preferential excitation of some minor centers and the neglect of reabsorption or saturation effects could lead to misleading information on the concentration and properties of these centers.

## ACKNOWLEDGMENTS

Some of the flux- or Bridgman-grown crystals used in this study were kindly supplied by Professor G. F. Imbusch from University College, Galway, Ireland and by Dr. A. Petrosyan from Institute of Physics of the Armenian Academy of Sciences, Yerevan, Armenia.

[1]D. P. Devor and L. G. DeShazer, Opt. Commun. **46**, 97 (1983).
[2]D. P. Devor, L. G. DeShazer, and R. C. Pastor, IEEE J. Quantum Electron. **25**, 1863 (1989).
[3]V. Lupei, A. Lupei, S. Georgescu, and W. M. Yen, J. Appl. Phys. **66**, 3792 (1989).
[4]S. Geller, G. P. Espinosa, L. D. Fullmer, and P. B. Crandall, Mater. Res. Bull. **7**, 1219 (1972).
[5]C. D. Brandle and L. R. Barns, J. Cryst. Growth **26**, 169 (1974).
[6]Yu. K. Voronko and A. A. Sobol, Phys. Status Solidi A **27**, 657 (1975).
[7]M. Kh. Ashurov, Yu. K. Voronko, A. A. Sobol, and M. I. Timoshechkin, Phys. Status Solidi A **42**, 101 (1977).
[8]V. V. Osiko, Yu. K. Voronko, and A. A. Sobol, *Crystals* (Springer-Verlag, Berlin, 1984), Vol. 10, p. 37.
[9]V. Lupei, A. Lupei, S. Georgescu, and C. Ionescu, Opt. Commun. **60**, 59 (1986).
[10]A. Lupei, V. Lupei, S. Georgescu, C. Ionescu, and W. M. Yen, J. Lumin. **39**, 36 (1987).
[11]J. Chenavas, J. C. Joubert, M. Marezio, and B. Ferrand, J. Less-Common Met. **62**, 373 (1978).
[12]Jun Dong and Kunquan Lu, Phys. Rev. B **43**, 8808 (1991).
[13]Zhonghua Wu, Kunquan Lu, Jun Dong, Fenyu Li, Zhengmin Fu, and Zhengzhi Fang, Z. Phys. B **82**, 15 (1991).
[14]R. W. Watts and W. C. Holton, J. Appl. Phys. **45**, 873 (1974).
[15]L. D. Merkle and R. C. Powell, Phys. Rev. B **20**, 75 (1979).
[16]G. E. Venikouas, G. J. Quarles, J. P. King, and R. C. Powell, Phys. Rev. B **30**, 2401 (1984).
[17]V. V. Grabovskii, A. F. Gumenyuk, V. Ya. Degoda, S. E. Zelenskii, and V. A. Okhrimenko, Opt. Spectrosc. **72**, 577 (1992).
[18]J. A. Mares, Z. Khas, W. Nie, and G. Boulon, J. Phys. I **1**, 881 (1991).
[19]V. Lupei, A. Lupei, S. Georgescu, and I. Ursu, Appl. Phys. Lett. **59**, 905 (1991).
[20]D. M. Gualtieri, P. F. Tumelty, and M. A. Gilleo, J. Appl. Phys. **52**, 2335 (1981).
[21]S. R. Rotman and F. X. Hartman, Chem. Phys. Lett. **152**, 311 (1988).
[22]M. Malinowski, P. Szczepanski, W. Wolinski, R. Wolski, and Z. Frukacz, J. Phys. Condens. Matter **5**, 6469 (1993).
[23]N. I. Agladze *et al.*, Kristallografiya **33**, 1400 (1988).
[24]V. Lupei, L. Lou, G. Boulon, and A. Lupei, J. Phys. Condens. Matter **5**, L35 (1993).
[25]J. Garcia Sole, A. Monteil, G. Boulon, E. Camarillo, J. O. Tocho, I. Vergara, and F. Jaque, J. Phys. IV (France) Colloq. **1**, C7-403 (1991).
[26]A. D. Dudka, A. A. Kaminskii, and V. I. Smirnov, Phys. Status Solidi A **93**, 495 (1985).